

Efficiency at maximum power of a Carnot quantum information engine

Paul Fadler,¹ Alexander Friedenberger,¹ and Eric Lutz²

¹*Department of Physics, Friedrich-Alexander-Universität Erlangen-Nürnberg, D-91058 Erlangen, Germany*

²*Institute for Theoretical Physics I, University of Stuttgart, D-70550 Stuttgart, Germany*

Optimizing the performance of thermal machines is an essential task of thermodynamics. We here consider the optimization of information engines that convert information about the state of a system into work. We concretely introduce a generalized finite-time Carnot cycle for a quantum information engine and optimize its power output in the regime of low dissipation. We derive a general formula for its efficiency at maximum power valid for arbitrary working media. We further investigate the optimal performance of a qubit information engine subjected to weak energy measurements.

Heat engines convert thermal energy into mechanical work by running cyclicly between two heat baths at different temperatures. They have been widely used to generate motion, from ancient steam engines to modern internal combustion motors [1]. Information engines, on the other hand, extract energy from a single heat bath by processing information, for instance, via cyclic measurement and feedback operations [2–14]. They thus exploit information gained about the state of a system to produce useful work [15, 16]. Such machines may be regarded as interacting with one heat reservoir and one information reservoir which only exchanges entropy, but no energy, with the device [17–19]. Information engines are possible owing to a fundamental connection between information and thermodynamics, as exemplified by Maxwell’s celebrated demon [20–22]. Successful information-to-work conversion has been reported in a growing number of classical experiments [24–34].

At low enough temperatures, typical nonclassical effects, such as coherent superposition of states and measurement back-action that randomly perturbs the state of a system, come into play [35]. They deeply affect the work extraction mechanism and impact the performance of measurement controlled quantum machines [36–44]. In this context, quantum measurements, in either their strong (projective) or weak (nonprojective) forms [35], may be considered as an unconventional thermodynamic resource [36–44]. Experimental investigations of the thermodynamic properties of a quantum Maxwell’s demon, based on quantum measurement and feedback control of a qubit system, have recently been performed using nuclear magnetic resonance [45] as well as superconducting [46–48] and cavity quantum electrodynamical [49] setups.

Two central performance measures of heat engines are efficiency, defined as the ratio of work output and heat input, and power that characterizes the work-output rate [1]. The efficiency of any heat engine coupled to thermal baths is bounded from above by the Carnot efficiency, $\eta_C = 1 - T_c/T_h$, where $T_{c,h}$ are the respective temperatures of the cold and hot heat reservoirs [1]. This value is usually only reachable in the ideal reversible limit, which corresponds to vanishing power. However, real thermal machines operate in finite time with finite power, and far from reversible conditions. Their efficiency is hence reduced by irreversible losses [50, 51]. Optimizing the

cyclic operation of heat engines is therefore crucial. A practical figure of merit is the efficiency at maximum power which has been extensively studied for classical [52–57] and quantum [58–62] heat engines. A general example of such an efficiency at maximum power is the Curzon-Ahlborn formula, $\eta_{CA} = 1 - \sqrt{T_c/T_h}$, which bears a striking resemblance to the Carnot expression, except for the square root [63]. The Curzon-Ahlborn efficiency appears to be universal for finite-time Carnot machines that operate under conditions of low, symmetric dissipation [55]. While information engines also run in finite time and with finite power, no generic expression for their efficiency at maximum power is currently known, owing to the difficulty to properly optimize them [11–13].

We here introduce a generalized Carnot cycle for a quantum information engine by replacing the cold heat bath of a finite-time quantum Carnot heat engine by an information reservoir. This cycle is fully reversible in the infinite-time limit. We optimize its power output and derive a general formula for the efficiency at maximum power for arbitrary working media within the framework of nonequilibrium thermodynamics in the weak dissipation regime. We obtain a Curzon-Ahlborn-like expression where the optimal cold coupling time is replaced by a new dissipation time that characterizes irreversible losses. We further illustrate our findings with the example of a qubit information engine, and obtain a microscopic expression of its efficiency at maximum power.

Reversible information engine cycle. The reversible Carnot cycle describes the most efficient heat engine, and is thus of fundamental importance. It consists of two adiabatic and of two isothermal (expansion and compression) branches [1]. Its realization requires two heat baths: a hot bath from which heat is absorbed during the hot isotherm and a cold bath which takes on heat during the cold isotherm. Finite-time quantum Carnot cycles have been theoretically studied in Refs. [64–68]. The first experimental implementation of a classical finite-time Carnot engine has been presented in Ref. [69]. We here construct a finite-time generalization of the Carnot cycle for a quantum information engine by substituting the cold heat bath (and the corresponding isotherm) by an information bath that involves measurement and subsequent outcome-dependent feedback (Fig. 1).

An important feature of this information cycle is that

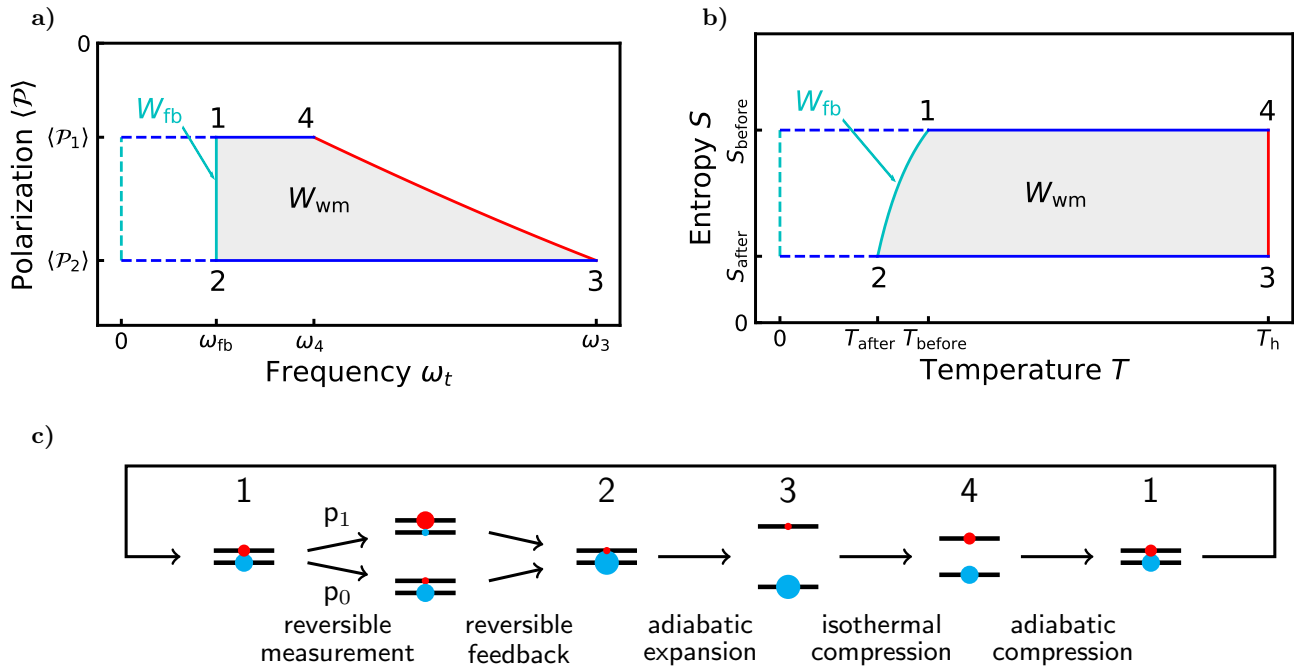


FIG. 1. Generalized finite-time Carnot cycle for the quantum information engine. a) Polarization-frequency diagram for an arbitrary working medium with Hamiltonian $H_t = \omega_t \mathcal{P}$. The cycle consists of one isochore during which a reversible measurement-plus-feedback protocol is implemented (1-2), one adiabatic expansion (2-3), one isothermal compression (3-2), and one adiabatic compression (4-1). The work $\langle W_{wm} \rangle$ produced by the working medium during one cycle is given by the enclosed area and the reversible feedback work $\langle W_{fb} \rangle$ is extracted during step (1-2). The total work done is equal to the sum $\langle W \rangle = \langle W_{wm} \rangle + \langle W_{fb} \rangle$. b) Entropy-temperature diagram of the same cycle. It reduces to a Carnot cycle for vanishing feedback frequency, $\omega_{fb} = 0$, (dashed lines). c) Explicit realization of the four steps of the cycle for a qubit information engine. The blue (red) dot represents the occupation probability of the ground (excited) state of the two-level system. The two outcomes of the reversible generalized energy measurement with Kraus operators (7) occur with respective probabilities (p_0, p_1) .

it is thermodynamically reversible for infinitely long cycle durations, like its thermal counterpart. In other words, each branch, including measurement and feedback, does not dissipate any irreversible entropy in that limit. We concretely impose the following three conditions on the engine cycle: (a) both measurement and feedback control are reversible, (b) the cycle is independent of the measurement outcome, meaning that measurement and feedback operation always lead to the same state, irrespective of the measurement result, and (c) the state ρ_{after} after measurement and feedback is a thermal state at temperature T_{after} with the same Hamiltonian H as that of the state ρ_{before} before the measurement.

We measure the state of the working medium of the information engine with a generalized measurement described by a set of positive operators $\{M_i\}$ that satisfy $\sum_i M_i^\dagger M_i = I$. The state after a measurement is $\rho_i = M_i \rho_{before} M_i^\dagger / p_i$ with probability $p_i = \text{Tr}[M_i \rho_{before} M_i^\dagger]$ [35]. We denote by $S_i = -k \text{Tr}[\rho_i \ln \rho_i]$ the entropy and by $E_i = \text{Tr}[\rho_i H]$ the energy of that state (k is the Boltzmann constant). Such a generalized measurement usually leads to a classical mixtures of states, implying that entropy is irreversibly produced during the process, $S(\rho_{meas}) > S(\rho_{before})$, where $\rho_{meas} = \sum_i p_i \rho_i$

is the density operator averaged over all the measurement outcomes, unless $[M_i, \rho_{before}] = 0$ [38]. In order to make the measurement thermodynamically reversible, $S(\rho_{meas}) = S(\rho_{before})$, we accordingly require that the operators M_i commute with the state of the system before the measurement, $[M_i, \rho_{before}] = 0$. Since the latter state is diagonal in the energy basis after the adiabatic compression branch, the operators M_i describe a nonprojective measurement of the energy of the working fluid. We next apply reversible feedback control [5] to transform each state ρ_i into the thermal state ρ_{after} . To that end, depending on the measurement outcome, we reversibly reorder the populations of ρ_i so that they decrease monotonically with increasing energy, while keeping the entropies S_i constant. We further shift the energy levels in order to obtain, after completion of the feedback operation, the same Hamilton operator as that of the initial state ρ_{before} . The explicit measurement-plus-feedback protocol for the case of a two-level system is detailed below.

The average entropy change provided by the measurement is $\langle \Delta S \rangle = \sum_i p_i S_i - S_{before} \leq 0$, where S_{before} is the entropy of state ρ_{before} before the measurement [35]. Noting that after feedback control, $\rho_i = \rho_{after}$ and, therefore,

$S_i = S_{\text{after}}$ for all measurement outcomes i , we simply have $\langle \Delta S \rangle = S_{\text{after}} - S_{\text{before}} = \Delta S$. The average work extracted by the reversibly operating feedback controller is additionally $\langle W_{\text{fb}} \rangle = \sum_i p_i (E_i - E_{\text{after}})$, since the individual entropies S_i remain constant during the feedback process. Furthermore, since $[M_i, \rho_{\text{before}}] = 0$, and hence $\sum_i p_i E_i = E_{\text{before}}$, we have $\langle W_{\text{fb}} \rangle = E_{\text{before}} - E_{\text{after}}$.

Let us now evaluate the work associated with the engine cycle shown in Fig. 1. For that purpose, it is useful to distinguish, on the one hand, the measurement and feedback part (step (1-2) in Fig. 1), as discussed above, and, on the other hand, the engine cycle seen from the standpoint of the working medium (steps (1-4) in Fig. 1) [70]. During adiabatic expansion and compression, the system is isolated from the bath. In order to make these steps reversible and avoid quantum friction [71–73], the Hamiltonian is chosen to commute with itself at all times, $[H_t, H_{t'}] = 0$, as in the standard quantum Carnot cycle [64–68]. As a result, nonadiabatic transitions do not occur for all driving times while work is performed. For concreteness, and without loss of generality, we consider a Hamilton operator of the scaling form $H_t = \omega_t \mathcal{P}$, with time-dependent frequency ω_t [68]. From the point of view of the working medium, the cycle then consists of four branches (Fig. 1): (1-2) one isochore at constant frequency ω_{fb} , (2-3) one adiabat with frequency variation from ω_{fb} to ω_3 , (3-4) one isotherm with frequency change from ω_3 to ω_4 at constant bath temperature T_h , and (4-1) one adiabat with frequency decrease from ω_4 to ω_{fb} . The average produced work $\langle W_{\text{wm}} \rangle$ is simply given by the area enclosed by the cycle. According to the first law applied to the working medium, we have $\langle W_{\text{wm}} \rangle = \langle Q_h \rangle + \langle Q_c \rangle$, where $\langle Q_{h,c} \rangle$ are the respective heat contributions from the isotherm and the isochore. In the long-time limit, the heat absorbed from the hot reservoir may be written in leading order (low dissipation regime) as $Q_h = T_h(\Delta S - \Sigma/\tau_h)$, where Σ is a coefficient that characterizes the entropy production during time τ_h along the isotherm [56]. Moreover, the heat exchanged by the working medium during the cold isochore can be evaluated by purely thermodynamic means (without involving the measurement and feedback aspect) [58–60]. It is given by $\langle Q_c \rangle = \omega_{\text{fb}} \Delta \langle \mathcal{P} \rangle = E_{\text{after}} - E_{\text{before}}$.

The total work $\langle W \rangle$ done during the complete information engine cycle is the sum of the work extracted by the feedback controller, $\langle W_{\text{fb}} \rangle$, and the work produced by the working medium, $\langle W_{\text{wm}} \rangle$. We hence obtain

$$\langle W \rangle = \langle W_{\text{fb}} \rangle + \langle W_{\text{wm}} \rangle = T_h \left(\Delta S - \frac{\Sigma}{\tau_h} \right). \quad (1)$$

We note that $\langle Q_c \rangle$ and $\langle W_{\text{fb}} \rangle$ exactly cancel. In other words, the information reservoir only exchanges entropy but no energy with the system. We are now in the position to investigate the phenomenological finite-time performance of the generalized Carnot information engine.

Efficiency at maximum power. The efficiency at which information is converted into work in the cyclic quantum

information engine is defined as [36–44]

$$\eta = \frac{\langle W \rangle}{T_h \Delta S} = 1 - \frac{\Sigma}{\Delta S \tau_h}, \quad (2)$$

where we have used Eq. (1). Unit efficiency ($\eta_{\text{max}} = 1$) is achieved for $\tau_h \rightarrow \infty$, when the cycle is reversible. In this regime, information about the state of the system, gained through the measurement, is fully converted into work by the cyclic engine. For finite-time operation, the efficiency is reduced ($\eta < 1$) owing to dissipative processes associated with irreversible entropy production.

The power of the information engine further reads [1]

$$P = \frac{\langle W \rangle}{\tau_h + \tau_{\text{fb}}} = \frac{T_h \left(\Delta S - \frac{\Sigma}{\tau_h} \right)}{\tau_h + \tau_{\text{fb}}}, \quad (3)$$

where τ_{fb} denotes the time of the measurement and feedback protocol. The time spent along the two adiabats can be set to zero since they are reversible irrespective of their duration [58, 59]. By contrast, the feedback time τ_{fb} is determined by the measurement-feedback process and we take it to be fixed [74]. Setting the derivative of the power P with respect to τ_h to zero, we find the optimal coupling time to the hot heat reservoir

$$\tau_h^* = \frac{\Sigma}{\Delta S} \left(1 + \sqrt{1 + \frac{\Delta S}{\Sigma} \tau_{\text{fb}}} \right). \quad (4)$$

The corresponding efficiency at maximum power η^* of the quantum information engine then follows as

$$\eta^* = 1 - \frac{1}{1 + \sqrt{1 + \tau_{\text{fb}}/\tau_h^{\otimes}}} = 1 - \frac{\tau_h^{\otimes}}{\tau_h^*}, \quad (5)$$

where we have used Eq. (4) and introduced the typical dissipation time $\tau_h^{\otimes} = \Sigma/\Delta S$ associated with irreversible losses along the hot isotherm: τ_h^{\otimes} is small (resp. large) when the entropy production is small (resp. large). Expression (5) is reminiscent of the Curzon-Ahlborn formula [63], which can be written in terms of the optimal cold and hot coupling times, τ_c^* and τ_h^* , as $\eta_{\text{CA}} = 1 - \tau_c^*/\tau_h^*$ [58]. The optimal time of the cold isotherm τ_c^* is here simply replaced by the new dissipation time τ_h^{\otimes} . We moreover observe from Eq. (5) that in general $\eta_{\text{max}}/2 < \eta^* < \eta_{\text{max}} = 1$, the lower (upper) bound being reached when the feedback time is much smaller (larger) than the dissipation time $\tau_{\text{fb}} \ll \tau_h^{\otimes}$ ($\tau_{\text{fb}} \gg \tau_h^{\otimes}$).

With the help of the above expressions, the maximum power P^* may furthermore be written as,

$$P^* = \frac{\eta^* T_h \Delta S}{\tau_h^* + \tau_{\text{fb}}}, \quad (6)$$

with the optimal produced work $\langle W \rangle^* = \eta^* T_h \Delta S$. These results generically hold for any working medium.

Qubit information engine. We proceed by illustrating our findings with the case of a spin-1/2 information engine with Hamilton operator $H_t = \omega_t \sigma_z/2 = \omega_t \mathcal{P}$, where

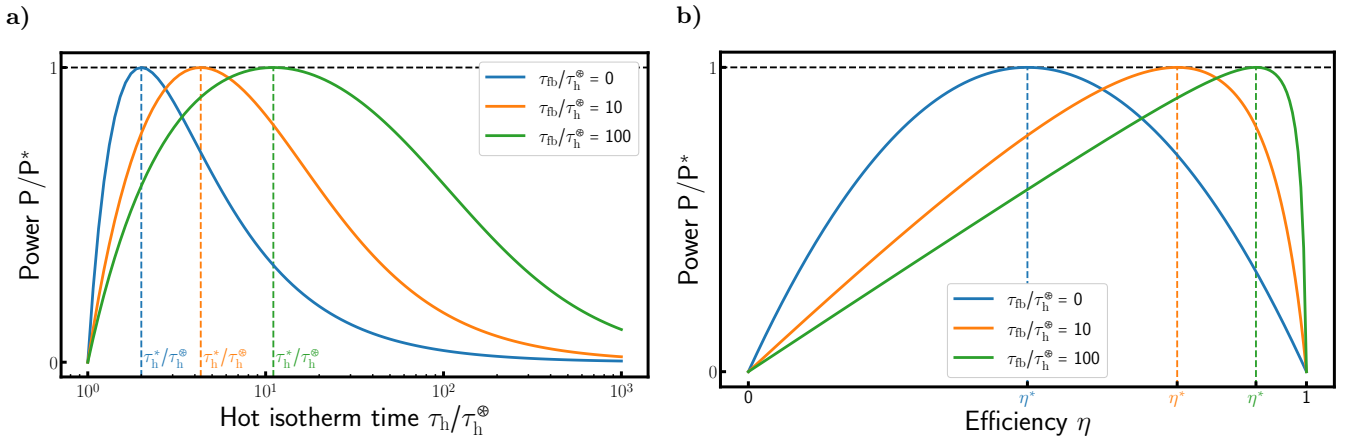


FIG. 2. Optimal performance of the quantum information engine. a) Reduced power P/P^* , Eq. (3), as a function of the duration of the hot isotherm τ_h , Eq. (4), for different values of the feedback time τ_{fb} (both in units of the dissipation time τ_h^{\otimes}). Maximum power P^* is reached at the optimal time τ_h^* . b) Power versus efficiency curves, for the same parameters, that exhibit the characteristic shape of an endoreversible engine. The general inequality $\eta_{\max}/2 < \eta^* < \eta_{\max} = 1$ is verified.

σ_z is the usual Pauli operator and $\mathcal{P} = \sigma_z/2$ is the polarization. The knowledge of the precise quantum dynamics of this system allows for the microscopic evaluation of the efficiency at maximum power of the information engine.

We begin by specifying the measurement-feedback protocol of the generalized finite-time Carnot cycle (Fig. 1). In order to satisfy the conditions (a)-(c) stated above (measurement and feedback should be reversible, all measurement results should be mapped onto the thermal state ρ_{after} with the same Hamilton operator as ρ_{before}), we construct a generalized quantum measurement such that the first measurement outcome ($i = 0$) is ρ_{after} (that is, $\rho_0 = \rho_{\text{after}}$ with energy $E_0 = E_{\text{after}}$) and the second measurement outcome ($i = 1$) is equal to its spin-flipped counterpart (that is, $\rho_1 = \sigma_x \rho_{\text{after}} \sigma_x$ with energy $E_1 = -E_{\text{after}}$). The corresponding measurement operators are explicitly given by (Supplemental Material [75])

$$\begin{aligned}
 M_0 &= \sqrt{\frac{1 - e^{(\beta_b + \beta_a)\omega_{fb}}}{1 - e^{2\beta_a\omega_{fb}}}} |1\rangle\langle 1| + \sqrt{\frac{1 - e^{-(\beta_b + \beta_a)\omega_{fb}}}{1 - e^{-2\beta_a\omega_{fb}}}} |0\rangle\langle 0| \\
 M_1 &= \sqrt{\frac{1 - e^{(\beta_b - \beta_a)\omega_{fb}}}{1 - e^{-2\beta_a\omega_{fb}}}} |1\rangle\langle 1| + \sqrt{\frac{1 - e^{-(\beta_b - \beta_a)\omega_{fb}}}{1 - e^{2\beta_a\omega_{fb}}}} |0\rangle\langle 0|
 \end{aligned} \quad (7)$$

where $\beta_b = \beta_{\text{before}}$ and $\beta_a = \beta_{\text{after}}$ are the respective inverse temperatures of the states ρ_{before} and ρ_{after} . The kets $|0\rangle$ and $|1\rangle$ denote the (ground and excited) energy eigenstates of the qubit. The Kraus operators (7) describe a nonprojective energy measurement of the spin-1/2 (it becomes weak in the high-temperature limit).

We next apply outcome-dependent feedback control to transform all the measurement results ($i = 0, 1$) into the same state ρ_{after} . For outcome 0, we apply the identity I , since $\rho_0 = \rho_{\text{after}}$ by construction; we hence trivially have $H_0 = H$. For outcome 1, we unitarily rearrange the states with the transformation $H_1 = -H + (E_1 - E_{\text{after}})I$, which

leaves the energy of the state unchanged, $\text{Tr}[\rho_1 H_1] = \text{Tr}[\rho_1 H]$. We finally shift the energy level to obtain the Hamiltonian of the state ρ_{before} . In doing so, we extract the feedback work $\langle W_{fb} \rangle = E_{\text{before}} - E_{\text{after}}$.

The interaction of the two-level system with the hot heat bath may be microscopically described with the help of a usual quantum master equation of the form [58, 59]

$$\begin{aligned}
 \dot{\mathcal{P}}_t &= \gamma_+ (\sigma_- [\mathcal{P}_t, \sigma_+] + [\sigma_-, \mathcal{P}_t] \sigma_+) \\
 &+ \gamma_- (\sigma_+ [\mathcal{P}_t, \sigma_-] + [\sigma_+, \mathcal{P}_t] \sigma_-) + \frac{\partial \mathcal{P}_t}{\partial t}, \quad (8)
 \end{aligned}$$

for the polarization \mathcal{P}_t in the Heisenberg picture and the operators $\sigma_{\pm} = \sigma_x \pm i\sigma_y$. Assuming that the damping coefficients satisfy the detailed-balance condition $\gamma_-/\gamma_+ = \exp(\beta_h \omega_t)$, by choosing, for instance, the concrete parametrization $\gamma_+ = a \exp(q\beta_h \omega_t)$ and $\gamma_- = a \exp((1+q)\beta_h \omega_t)$ (with $a > 0$ and $0 > q > -1$ constant parameters), Eq. (8) can be rewritten as [58, 59]

$$\langle \dot{\mathcal{P}}_t \rangle = -a e^{q\beta_h \omega_t} [2(1 + e^{\beta_h \omega_t}) \langle \mathcal{P}_t \rangle + (e^{\beta_h \omega_t} - 1)]. \quad (9)$$

The parameter a characterizes the magnitude of the damping coefficients and, thus, the rate of change of the average polarization. Solving the above equation for time [58, 59], the duration of the isotherm in the high-temperature limit ($\beta_h \omega_{3,4} \ll 1$) is found to read [75]

$$\tau_h = \frac{\ln(\omega_3/\omega_4)}{4a(1 - \beta_h/\beta')}, \quad (10)$$

where the effective inverse temperature β' of the qubit is determined via $\langle \mathcal{P}_t \rangle = -\tanh(\beta' \omega_t/2)/2$ [58, 59]. Due to the finite-time relaxation of the system, the temperature T' is not necessarily equal to the bath temperature T_h , when thermalization is not complete; we have $\tau_h \rightarrow \infty$ when $T' \rightarrow T_h$ (or $a \rightarrow 0$). Noting further that the work

$\langle W \rangle = T_h(\Delta S - \Sigma/\tau_h)$ produced by the irreversible engine cycle with bath temperature T_h is equal to the work $T'\Delta S$ produced by a reversible cycle with effective bath temperature T' [58], we find the dissipation time,

$$\tau_h^\otimes = \frac{\Sigma}{\Delta S} = \frac{\ln(\omega_3/\omega_4)}{4a}. \quad (11)$$

Equation (11) is solely determined by the beginning and end frequencies $\omega_{3,4}$ of the isotherm and the bath coupling parameter a . We therefore obtain the microscopic expression for the efficiency at maximum power (5):

$$\eta^* = 1 - \frac{\tau_h^\otimes}{\tau_h^*} = 1 - \frac{1}{1 + \sqrt{1 + 4a\tau_{fb}/\ln(\omega_3/\omega_4)}}. \quad (12)$$

Figure 2a) displays the reduced power P/P^* of the qubit information engine as a function of the duration of the hot isotherm τ_h for different values of the feedback time τ_{fb} (both in units of τ_h^\otimes). We identify a clear maximum at the optimal time τ_h^* given by Eq. (4). Figure 2b) moreover shows the corresponding power versus efficiency curves that are typical for an endoreversible engine [52]. Such machines are internally reversible and irreversible losses only occur via thermal contact with the external bath. They hence outperform fully irreversible engines and have played for this reason a central role in finite-time thermodynamics [50, 51]. We note that the general inequality $\eta_{\max}/2 < \eta^* < \eta_{\max} = 1$ is satisfied.

Conclusions. We have proposed a generalized finite-time Carnot cycle for a quantum information engine. Like the standard Carnot cycle for heat engines, it is thermodynamically reversible for large cycle durations. This cycle thus describes the most efficient quantum information engine with unit information efficiency. We have optimized its power output in the regime of low dissipation and derived a Curzon-Ahlborn-like formula for its efficiency at maximum power. This generic expression only depends on the optimal time of the hot isotherm and a new dissipation time associated with irreversible entropy production. The efficiency at maximum power was further shown to obey the general inequality $1/2 < \eta^* < 1$, independent of the microscopic details of the engine. Our results provide a theoretical basis for the optimization of information engines. We hence expect them to be important for the study of optimal quantum machines in finite-time information thermodynamics.

ACKNOWLEDGMENTS

We acknowledge financial assistance from the German Science Foundation (DFG) (under project FOR 2724) and thank Florian Marquardt for his support.

-
- [1] Y. A. Cengel and M. A. Boles, *Thermodynamics. An Engineering Approach*, (McGraw-Hill, New York, 2001).
 - [2] F. J. Cao and M. Feito, Thermodynamics of feedback controlled systems, *Phys. Rev. E* **79**, 041118 (2009).
 - [3] T. Sagawa and M. Ueda, Generalized Jarzynski Equality under Nonequilibrium Feedback Control, *Phys. Rev. Lett.* **104**, 090602 (2010).
 - [4] D. Abreu and U. Seifert, Extracting Work from a Single Heat Bath through Feedback, *EPL* **94**, 10001 (2011).
 - [5] J. M. Horowitz and J. M. R. Parrondo, Thermodynamic reversibility in feedback processes, *EPL* **95**, 10005 (2011).
 - [6] M. Bauer, D. Abreu and U. Seifert, Efficiency of a Brownian information machine, *J. Phys. A* **45**, 162001 (2012).
 - [7] T. Sagawa and M. Ueda, Nonequilibrium thermodynamics of feedback control, *Phys. Rev. E* **85**, 021104 (2012).
 - [8] M. Esposito and G. Schaller, Stochastic thermodynamics for "Maxwell demon" feedbacks, *EPL* **99**, 30003 (2012).
 - [9] D. Mandal, H. T. Quan, and C. Jarzynski, Maxwell's Refrigerator: An Exactly Solvable Model, *Phys. Rev. Lett.* **111**, 030602 (2013).
 - [10] J. M. Horowitz, T. Sagawa, and J. M. R. Parrondo, Imitating Chemical Motors with Optimal Information Motors, *Phys. Rev. Lett.* **111**, 010602 (2013).
 - [11] J. Um, H. Hinrichsen, C. Kwon, and H. Park, Total cost of operating an information engine, *New J. Phys.* **17**, 085001 (2015).
 - [12] J. M. Park, J. S. Lee, and J. D. Noh, Optimal tuning of a confined Brownian information engine, *Phys. Rev. E* **93**, 032146 (2016).
 - [13] S. Yamamoto, S. Ito, N. Shiraishi, and T. Sagawa, Linear irreversible thermodynamics and Onsager reciprocity for information-driven engines, *Phys. Rev. E* **94**, 052121 (2016).
 - [14] J. M. Horowitz and J. M. R. Parrondo, Designing optimal discrete-feedback thermodynamic engines, *New J. Phys.* **13**, 123019 (2019).
 - [15] U. Seifert, Stochastic thermodynamics, fluctuation theorems and molecular machines, *Rep. Prog. Phys.* **75**, 126001 (2012).
 - [16] T. Sagawa, Thermodynamics of information processing in small systems, *Prog. Theor. Phys.* **127**, 1 (2012).
 - [17] S. Deffner and C. Jarzynski, Information Processing and the Second Law of Thermodynamics: An Inclusive, Hamiltonian Approach, *Phys. Rev. X* **3**, 041003 (2013).
 - [18] A. C. Barato and U. Seifert, Unifying Three Perspectives on Information Processing in Stochastic Thermodynamics, *Phys. Rev. Lett.* **112**, 090601 (2014).
 - [19] A. C. Barato and U. Seifert, Stochastic thermodynamics with information reservoirs, *Phys. Rev. E* **90**, 042150 (2014).
 - [20] J. M. Parrondo, J. M. Horowitz, and T. Sagawa, Thermodynamics of information, *Nature Phys.* **11**, 131 (2015).
 - [21] E. Lutz and S. Ciliberto, Information: From Maxwell's demon to Landauer's eraser, *Phys. Today* **68**, 30 (2015).
 - [22] K. Maruyama, F. Nori, and V. Vedral, Colloquium: The physics of Maxwell's demon and information, *Rev. Mod. Phys.* **81**, 011001 (2009).

- Phys. **81**, 1 (2009).
- [23] M. G. Raizen, Comprehensive Control of Atomic Motion, Science **324**, 1403 (2009).
- [24] S. Toyabe, T. Sagawa, M. Ueda, E. Muneyuki, and M. Sano, Experimental demonstration of information-to-energy conversion and validation of the generalized Jarzynski equality, Nature Phys. **6**, 988 (2010).
- [25] E. Roldan, I. A. Martinez, J. M. R. Parrondo, and D. Petrov, Universal features in the energetics of symmetry breaking, Nature Phys. **10**, 457 (2014).
- [26] J. V. Koski, V. F. Maisi, J. P. Pekola, and D. V. Averin, Experimental realization of a Szilard engine with a single electron, Proc. Natl. Acad. Sci. U.S.A. **111**, 13786 (2014).
- [27] J. V. Koski, V. F. Maisi, T. Sagawa, and J. P. Pekola, Experimental Observation of the Role of Mutual Information in the Nonequilibrium Dynamics of a Maxwell Demon, Phys. Rev. Lett. **113**, 030601 (2014).
- [28] J. V. Koski, A. Kutvonen, I. M. Khaymovich, T. Ala-Nissila, and J. P. Pekola, On-Chip Maxwell's Demon as an Information-Powered Refrigerator, Phys. Rev. Lett. **115**, 260602 (2015).
- [29] M. D. Vidrighin, O. Dahlsten, M. Barbieri, M. S. Kim, V. Vedral, and I. A. Walmsley, Photonic Maxwell's Demon, Phys. Rev. Lett. **116**, 050401 (2016).
- [30] K. Chida, S. Desai, K. Nishiguchi, and A. Fujiwara, Power generator driven by Maxwell's demon, Nature Commun. **8**, 15310 (2017).
- [31] M. Ribezzi-Crivellari and F. Ritort, Large work extraction and the Landauer limit in a continuous Maxwell demon, Nature Phys. **15**, 660 (2019).
- [32] G. Paneru, D. Y. Lee, T. Thusty, and H. K. Pak, Lossless Brownian Information Engine, Phys. Rev. Lett. **120**, 020601 (2018).
- [33] T. Admon, S. Rahav, and Y. Roichman, Experimental Realization of an Information Machine with Tunable Temporal Correlations, Phys. Rev. Lett. **121**, 180601 (2018).
- [34] G. Paneru, S. Dutta, T. Sagawa, T. Thusty, and H. K. Pak, Efficiency fluctuations and noise induced refrigerator-to-heater transition in information engines, Nature Commun. **11**, 1012 (2020).
- [35] K. Jacobs, *Quantum Measurement Theory*, (Cambridge University Press, Cambridge, 2014).
- [36] S. Lloyd, Quantum-mechanical Maxwell's demon, Phys. Rev. A **56**, 3374 (1997).
- [37] H. T. Quan, Y. D. Wang, Yu-xi Liu, C. P. Sun, and F. Nori, Maxwell's Demon Assisted Thermodynamic Cycle in Superconducting Quantum Circuits, Phys. Rev. Lett. **97**, 180402 (2006).
- [38] K. Jacobs, Second law of thermodynamics and quantum feedback control: Maxwell's demon with weak measurements, Phys. Rev. A **80**, 012322 (2009).
- [39] S. W. Kim, T. Sagawa, S. De Liberato, and M. Ueda, Quantum Szilard Engine, Phys. Rev. Lett. **106**, 070401 (2011).
- [40] P. Strasberg, G. Schaller, T. Brandes, and M. Esposito, Thermodynamics of a Physical Model Implementing a Maxwell Demon, Phys. Rev. Lett. **110**, 040601 (2013).
- [41] K. Brandner, M. Bauer, M. T. Schmid and U. Seifert, Coherence-enhanced efficiency of feedback-driven quantum engines, New J. Phys. **17**, 065006 (2015).
- [42] C. Elouard, D. Herrera-Marti, Benjamin Huard, and Alexia Auffèves, Extracting Work from Quantum Measurement in Maxwell's Demon Engines, Phys. Rev. Lett. **118**, 260603 (2017).
- [43] C. Elouard and A. N. Jordan, Efficient Quantum Measurement Engines, Phys. Rev. Lett. **120**, 260601 (2018).
- [44] S. Seah, S. Nimmrichter, and V. Scarani, Maxwell's Lesser Demon: A Quantum Engine Driven by Pointer Measurements, Phys. Rev. Lett. **124**, 100603 (2020).
- [45] P. A. Camati, J. P. S. Peterson, T. B. Batalho, K. Micadei, A. M. Souza, R. S. Sarthour, I. S. Oliveira, and R. M. Serra, Experimental Rectification of Entropy Production by Maxwell's Demon in a Quantum System, Phys. Rev. Lett. **117**, 240502 (2016).
- [46] N. Cottet, S. Jezouin, L. Bretheau, P. Campagne-Ibarcq, Q. Ficheux, J. Anders, A. Auffèves, R. Azouit, P. Rouchon, and B. Huard, Observing a quantum Maxwell demon at work, Proc. Natl. Acad. Sci. U.S.A. **114**, 7561 (2017).
- [47] Y. Masuyama, K. Funo, Y. Murashita, A. Noguchi, S. Kono, Y. Tabuchi, R. Yamazaki, M. Ueda, and Y. Nakamura, Information-to-work conversion by Maxwell's demon in a superconducting circuit quantum electrodynamical system, Nature Commun. **9**, 1291 (2018).
- [48] M. Naghiloo, J. J. Alonso, A. Romito, E. Lutz, and K. W. Murch, Information Gain and Loss for a Quantum Maxwell's Demon, Phys. Rev. Lett. **121**, 030604 (2018).
- [49] B.-L. Najera-Santos, P. A. Camati, V. Métillon, M. Brune, J.-M. Raimond, A. Auffèves, and I. Dotsenko, Autonomous Maxwell's demon in a cavity QED system, Phys. Rev. Research **2**, 032025 (2020).
- [50] B. Andresen, P. Salamon, and R. S. Berry, Thermodynamics in finite time, Phys. Today **37**, 62 (1984).
- [51] B. Andresen, Current trends in finite-time thermodynamics, Angew. Chem. Int. Ed. **50**, 2690 (2011).
- [52] J. Chen, The maximum power output and maximum efficiency of an irreversible Carnot heat engine, J. Phys. D: Appl. Phys. **27**, 1144 (1994).
- [53] C. Van den Broeck, Thermodynamic Efficiency at Maximum Power, Phys. Rev. Lett. **95**, 190602 (2005).
- [54] T. Schmiedl and U. Seifert, Efficiency at maximum power: an analytically solvable model for stochastic heat engines, EPL **81**, 20003 (2007).
- [55] M. Esposito, K. Lindenberg, and C. Van den Broeck, Universality of Efficiency at Maximum Power, Phys. Rev. Lett. **102**, 130602 (2009).
- [56] M. Esposito, R. Kawai, K. Lindenberg, and C. Van den Broeck, Efficiency at Maximum Power of Low-Dissipation Carnot Engines, Phys. Rev. Lett. **105**, 150603 (2010).
- [57] K. Proesmans, B. Cleuren, and C. Van den Broeck, Power-Efficiency-Dissipation Relations in Linear Thermodynamics, Phys. Rev. Lett. **116**, 220601 (2016).
- [58] E. Geva and R. Kosloff, A quantum-mechanical heat engine operating in finite time. A model consisting of spin-1/2 systems as the working fluid, J. Chem. Phys. **96**, 3054 (1992).
- [59] B. Lin and J. Chen, Optimal analysis of the performance of an irreversible quantum heat engine with spin systems, J. Phys. A: Math. Gen. **38**, 69 (2005).
- [60] J. Wang, J. He, and Z. Wu, Efficiency at maximum power output of quantum heat engines under finite-time operation, Phys. Rev. E **85**, 031145 (2012).
- [61] O. Abah, J. Roßnagel, G. Jacob, S. Deffner, F. Schmidt-Kaler, K. Singer, and E. Lutz, Single-Ion Heat Engine at Maximum Power, Phys. Rev. Lett. **109**, 203006 (2012).
- [62] J. Roßnagel, O. Abah, F. Schmidt-Kaler, K. Singer,

- and E. Lutz, Nanoscale Heat Engine Beyond the Carnot Limit, *Phys. Rev. Lett.* **112**, 030602 (2014).
- [63] F. L. Curzon and B. Ahlborn, Efficiency of a Carnot engine at maximum power output, *Am. J. Phys.* **43**, 22 (1975).
- [64] H. T. Quan, Y. Liu, C. P. Sun, F. Nori, Quantum thermodynamic cycles and quantum heat engines, *Phys. Rev. E* **76**, 031105 (2007).
- [65] S. Abe, Maximum-power quantum-mechanical Carnot engine, *Phys. Rev. E* **83**, 041117 (2011).
- [66] R. D. Dann and R. Kosloff, Quantum signatures in the quantum Carnot cycle, *New J. Phys.* **22**, 013055 (2020).
- [67] P. Abiuso and M. Perarnau-Llobet, Optimal Cycles for Low-Dissipation Heat Engines, *Phys. Rev. Lett.* **124**, 110606 (2020).
- [68] T. Denzler and E. Lutz, Power fluctuations in a finite-time quantum Carnot engine, *Phys. Rev. Research* **3**, 032041 (2021).
- [69] I. A. Martinez, E. Roldan, L. Dinis, D. Petrov, J. M. R. Parrondo and R. A. Rica, Brownian Carnot engine, *Nature Phys.* **12**, 67 (2015).
- [70] An alternative, but equivalent, analysis, where the measurement is treated separately, and the feedback operation, together with the remaining part of the cycle, is seen as the action of a controller, is presented in the Supplemental Material [75].
- [71] R. Kosloff and T. Feldmann, Discrete four-stroke quantum heat engine exploring the origin of friction, *Phys. Rev. E* **65**, 055102(R) (2002).
- [72] T. Feldmann and R. Kosloff, Quantum four-stroke heat engine: Thermodynamic observables in a model with intrinsic friction, *Phys. Rev. E* **68**, 016101 (2003).
- [73] F. Plastina, A. Alecce, T. J. G. Apollaro, G. Falcone, G. Francica, F. Galve, N. Lo Gullo, and R. Zambrini, Irreversible Work and Inner Friction in Quantum Thermodynamic Processes, *Phys. Rev. Lett.* **113**, 260601 (2014).
- [74] The optimization of the power P with respect to the feedback time τ_{fb} leads to a trivial zero solution.
- [75] See Supplemental Material.

Appendix A: Alternative thermodynamic analysis

Instead of performing the thermodynamic analysis of the finite-time quantum information engine as done in the main text by distinguishing, on the one hand, the measurement and feedback part (step (1-2) in Fig. 1), and, on the other hand, the engine cycle seen from the standpoint of the working medium (steps (1-4) in Fig. 1), we here present an alternative, but, equivalent, description that separates the measurement in point 1 in Fig. 1 and the remaining cycle which is now considered to be operated by a general controller. The latter cycle includes the feedback part that is conditioned on the measurement outcome, as well as the two adiabats and the isotherm (steps (1-4) in Fig. 1). This derivation generalizes the one discussed in Ref. [41] for a different quantum information cycle through the usage of incomplete measurements.

We begin by evaluating the respective changes of energy and entropy associated with (i) the measurement and with (ii) the remaining cycle. We have

$$\Delta E^{\text{meas}}(m) = E[\rho_m] - E[\rho_1] \quad (\text{A1})$$

$$\Delta S_{\text{sys}}^{\text{meas}}(m) = S_{\text{sys}}[\rho_m] - S_{\text{sys}}[\rho_1] \quad (\text{A2})$$

for the measurement with outcome m , and

$$\Delta E^{\text{cyc}}(m) = E[\rho_1] - E[\rho_m] \quad (\text{A3})$$

$$\Delta S_{\text{sys}}^{\text{cyc}}(m) = S_{\text{sys}}[\rho_1] - S_{\text{sys}}[\rho_m] \quad (\text{A4})$$

for the cycle implemented by the controller. The total entropy production during the cycle is the sum of the entropy change of the system and of the bath

$$\Delta S_{\text{tot}}^{\text{cyc}}(m) = \Delta S_{\text{sys}}^{\text{cyc}}(m) + \Delta S_{\text{bath}} \geq 0, \quad (\text{A5})$$

since the total entropy production is non-negative. We accordingly obtain

$$Q_{\text{h}} = Q(m) = -T\Delta S_{\text{bath}} \leq T\Delta S_{\text{sys}}^{\text{cyc}}(m). \quad (\text{A6})$$

The first law applied to the complete control operation then reads

$$\Delta E^{\text{cyc}}(m) = Q(m) - W(m) = Q_{\text{h}} - W, \quad (\text{A7})$$

or, equivalently,

$$W(m) \leq T\Delta S_{\text{sys}}^{\text{cyc}}(m) - \Delta E^{\text{cyc}}(m). \quad (\text{A8})$$

Since the measurement is reversible, that is, $S[\rho_m] = S[\rho_2]$ for all m , averaging $\Delta E^{\text{cyc}}(m)$ yields

$$\langle \Delta E^{\text{cyc}} \rangle = \sum_m p_m (E[\rho_1] - E[\rho_m]) = E[\rho_1] - \sum_m p_m \text{Tr}(H\rho_m) = E[\rho_1] - \sum_m p_m \text{Tr}\left(H \frac{M_m \rho_1 M_m^\dagger}{p_m}\right) \quad (\text{A9})$$

$$= E[\rho_1] - \text{Tr}\left(H\rho_1 \sum_m M_m^\dagger M_m\right) = E[\rho_1] - \text{Tr}(H\rho_1) = 0, \quad (\text{A10})$$

where we have used $[H, M_m] = 0$ and $\sum_m M_m^\dagger M_m = 1$. Similarly, we have $\langle \Delta E^{\text{meas}} \rangle = 0$. Since $\Delta S_{\text{sys}}^{\text{meas}} = -\Delta S_{\text{sys}}^{\text{cyc}} = S_{\text{sys}}[\rho_2] - S_{\text{sys}}[\rho_1]$, we eventually arrive at

$$\langle W \rangle \leq -T\Delta S_{\text{sys}}^{\text{meas}} = -T(S[\rho_2] - S[\rho_1]). \quad (\text{A11})$$

In the low dissipation limit, we may be further write the entropy production in the form

$$\frac{\Sigma}{\tau_h} = \Delta S_{\text{sys}}^{\text{cyc}}(m) + \Delta S_{\text{bath}}(m), \quad (\text{A12})$$

from which we find

$$Q_h = -Q(m) = -T\Delta S_{\text{bath}}(m) = T\left(\Delta S_{\text{sys}}^{\text{cyc}}(m) - \frac{\Sigma}{\tau_h}\right) \quad (\text{A13})$$

Combining everything, we finally obtain (denoting $\Delta S_{\text{sys}}^{\text{cyc}} = \Delta S$, as in the main text)

$$\langle W \rangle = T\left(\Delta S - \frac{\Sigma}{\tau_h}\right). \quad (\text{A14})$$

This is equation (1) of the main text.

Appendix B: Measurement operators for the qubit information engine

We here explicitly derive the Kraus operators M_i for the generalized quantum measurement implemented in the two-level information engine. They have to fulfill the condition

$$\rho_{\text{after}} = \Phi_i[\rho_i], \quad (\text{B1})$$

where the state ρ_{after} (after measurement and feedback) is a thermal state at effective temperature T_{after} and $\rho_i = M_i \rho_{\text{before}} M_i^\dagger / p_i$ is the state of the system after a measurement with outcome $i = (0, 1)$. For $i = 0$, $\Phi_0 = I$ is the identity, whereas for $i = 1$, $\Phi_1 = \Phi_{\text{flip}}$ is the quantum bit flip channel.

Let us parametrize the thermal states before and after the measurement as

$$\rho_{\text{before}} = \alpha |1\rangle\langle 1| + (1 - \alpha) |0\rangle\langle 0|, \quad (\text{B2})$$

$$\rho_{\text{after}} = \beta |1\rangle\langle 1| + (1 - \beta) |0\rangle\langle 0|. \quad (\text{B3})$$

Since the operators M_i commute with thermal states, we can also parametrize them by their diagonal entries as

$$M_0 = x |1\rangle\langle 1| + y |0\rangle\langle 0|, \quad (\text{B4})$$

$$M_1 = u |1\rangle\langle 1| + v |0\rangle\langle 0|. \quad (\text{B5})$$

Neglecting arbitrary phases by choosing $(x, y, u, v) \in \mathbb{R}^+$, which can always be done by properly adjusting the adiabatic protocol, we can eliminate the parameters u and v by using

$$\mathbb{1} = M_0^\dagger M_0 + M_1^\dagger M_1 = (x^* x + u^* u) |1\rangle\langle 1| + (y^* y + v^* v) |0\rangle\langle 0|. \quad (\text{B6})$$

We then obtain

$$u = \sqrt{1 - x^2} \quad \text{and} \quad v = \sqrt{1 - y^2}. \quad (\text{B7})$$

Looking at measurement outcome 0, we further have

$$\frac{M_0 \rho_{\text{before}} M_0^\dagger}{\text{Tr}(M_0 \rho_{\text{before}} M_0^\dagger)} = \rho_{\text{after}}, \quad (\text{B8})$$

or, explicitly

$$\frac{x^2 \alpha}{x^2 \alpha + y^2 (1 - \alpha)} |1\rangle \langle 1| + \frac{y^2 (1 - \alpha)}{x^2 \alpha + y^2 (1 - \alpha)} |0\rangle \langle 0| = \beta |1\rangle \langle 1| + (1 - \beta) |0\rangle \langle 0|. \quad (\text{B9})$$

Setting the populations of the excited state to be equal, we find

$$\frac{x^2 \alpha}{x^2 \alpha + y^2 (1 - \alpha)} = \beta. \quad (\text{B10})$$

The equality of the populations of the ground state is automatically fulfilled owing to the unit trace. On the other hand, looking at measurement outcome 1, we have

$$\frac{M_1 \rho_{\text{before}} M_1^\dagger}{\text{Tr}(M_1 \rho_{\text{before}} M_1^\dagger)} = \Phi_{\text{flip}}[\rho_{\text{after}}], \quad (\text{B11})$$

which leads to the equation

$$\frac{(1 - x^2) \alpha}{(1 - x^2) \alpha + (1 - y^2) (1 - \alpha)} = 1 - \beta. \quad (\text{B12})$$

Solving the set of Eqs. (B10) and (B12), we obtain

$$x = \sqrt{\frac{\beta - \beta^2 - \alpha \beta}{\alpha - 2\alpha \beta}} \quad \text{and} \quad y = \sqrt{\frac{1 - \beta}{1 - \alpha} \frac{1 - \beta - \alpha}{1 - 2\beta}}, \quad (\text{B13})$$

as well as

$$u = \sqrt{1 - \beta \frac{1 - \beta - \alpha}{\alpha - 2\alpha \beta}} \quad \text{and} \quad v = \sqrt{1 - \frac{1 - \beta}{1 - \alpha} \frac{1 - \beta - \alpha}{1 - 2\beta}}. \quad (\text{B14})$$

Writing further $\alpha = \frac{1}{1 + e^a}$ and $\beta = \frac{1}{1 + e^b}$, with $a = \beta_b \omega_{\text{fb}}$ and $b = \beta_a \omega_{\text{fb}}$, where $\beta_a = \beta_{\text{after}}$ is the inverse temperature of state ρ_{after} and $\beta_b = \beta_{\text{before}}$ is the inverse temperature of state ρ_{before} , we finally arrive at

$$x = \sqrt{\frac{e^{a+b} - 1}{e^{2b} - 1}}, \quad y = \sqrt{\frac{1 - e^{-a-b}}{1 - e^{-2b}}}, \quad u = \sqrt{\frac{1 - e^{-a-b}}{1 - e^{-2b}}} \quad \text{and} \quad v = \sqrt{\frac{e^{-a+b} + 1}{e^{2b} - 1}}. \quad (\text{B15})$$

Appendix C: Hot isotherm time for the qubit information engine

We next derive Eq. (10) of the main text for the duration of the hot isotherm following Refs. [58, 59]. We begin with Eq. (9) of the main text for the average polarization \mathcal{P}_t in the Heisenberg picture

$$\langle \dot{\mathcal{P}}_t \rangle = -a e^{q\beta\omega_t} [2(1 + e^{\beta\omega_t}) \langle \mathcal{P}_t \rangle + (e^{\beta\omega_t} - 1)]. \quad (\text{C1})$$

Applying the chain rule for derivatives, we have

$$\langle \dot{\mathcal{P}}_t \rangle = \frac{d \langle \mathcal{P}_t(\omega_t) \rangle}{d\omega_t} \frac{d\omega_t}{dt}. \quad (\text{C2})$$

Since the effective temperature along the isothermal branch is constant, we obtain from $\langle \mathcal{P}_t(\omega_t) \rangle = -\tanh(\beta' \omega_t / 2) / 2$

$$\frac{d \langle \mathcal{P}_t \rangle}{d\omega_t} = -\frac{\beta'}{2[\cosh(\beta' \omega_t) + 1]}. \quad (\text{C3})$$

Combining both equations, we obtain

$$\frac{d\langle \mathcal{P}_t \rangle}{d\omega_t} \frac{d\omega_t}{dt} = -ae^{q\beta_h\omega_t} [-(1 + e^{\beta_h\omega_t}) \tanh(\beta'\omega_t/2) + e^{\beta_h\omega_t} - 1]. \quad (\text{C4})$$

or, equivalently, solving for dt

$$dt = -\frac{(d\langle \mathcal{P}_t \rangle/d\omega_t)}{ae^{q\beta_h\omega_t} [-(1 + e^{\beta_h\omega_t}) \tanh(\beta'\omega_t/2) + (e^{\beta_h\omega_t} - 1)]} d\omega_t, \quad (\text{C5})$$

$$t = \frac{1}{2a} \int_{x_0}^{x(t)} [e^{q\epsilon x} (e^{\epsilon x} - e^{-x})(1 + e^{-x})]^{-1} dx, \quad (\text{C6})$$

where we have introduced the new variable $x = \beta'\omega_t$ and defined $\epsilon = \beta_h/\beta'$. Using the expansion $e^x \simeq 1 + x$ in the high-temperature limit, we finally arrive at

$$t = \frac{1}{2a} \int_{x_0}^{x_t} \frac{dx}{(1 + q\epsilon x)(1 + \epsilon x - (1 + x))(1 + 1 - x)} = \frac{\ln(\omega_3/\omega_4)}{4a(1 - \beta_h/\beta')}. \quad (\text{C7})$$

Appendix D: Entropy production for the qubit information engine

We finally derive an expression for the parameter Σ which determines the nonequilibrium entropy production. We consider an arbitrary N -dimensional working fluid with Hamilton operator $\mathcal{H}_t = \omega_t \mathcal{P} = \omega_t \sum_n \lambda_n |n\rangle \langle n|$. We choose the global energy offset of \mathcal{P} such that

$$\sum_n \lambda_n = 0 \quad \text{and} \quad \sum_n \lambda_n^2 = 2\chi. \quad (\text{D1})$$

In the high temperature limit ($\beta\lambda_n\omega_t \ll 1$), we can express the thermal state as

$$\rho = \frac{e^{-\beta\omega_t \mathcal{P}}}{\text{Tr}[e^{-\beta\omega_t \mathcal{P}}]} \simeq \frac{(1 - \beta\omega_t\lambda_N + (\beta\omega_t\lambda_N)^2/2) |N\rangle \langle N|}{Z}, \quad (\text{D2})$$

with the partition function

$$Z \simeq \sum_n [1 - \beta\omega_t\lambda_n + (\beta\omega_t\lambda_n)^2/2] = N - \beta\omega_t \sum_n \lambda_n + \beta^2\omega_t^2 \sum_n \lambda_n^2/2 = N + \beta^2\omega_t^2\chi. \quad (\text{D3})$$

The occupation probabilities are therefore

$$P_n = \langle n | \rho | n \rangle \simeq \frac{1 - \beta\omega_t\lambda_n + \beta^2\omega_t^2\lambda_n^2/2}{N + \beta^2\omega_t^2\chi} = \frac{1}{N} - \frac{\beta\omega_t\lambda_n}{N} + \frac{\beta^2\omega_t^2\lambda_n^2}{2N} - \frac{\beta^2\omega_t^2\chi}{N^2}. \quad (\text{D4})$$

The entropy can accordingly be written as

$$S = -\text{Tr}[\rho \ln \rho] = -\sum_n P_n \ln P_n \simeq \ln N - \frac{\beta^2\omega_t^2\chi}{N}. \quad (\text{D5})$$

The entropy changes for an isochoric process from β_1 to β_2 at frequency ω_t and an isothermal transformation from β_1 to β_2 at inverse temperature β thus read

$$\Delta S_{\text{isochoric}} = \frac{\omega_t^2\chi}{N} (\beta_2^2 - \beta_1^2) \quad \text{and} \quad \Delta S_{\text{isothermal}} = \frac{\beta^2\chi}{N} (\omega_2^2 - \omega_1^2). \quad (\text{D6})$$

The dissipation constant Σ for a two-level system (with $N = 2$ and $\chi = 1/4$) hence follows as

$$\Sigma = \Delta S \frac{\ln(\omega_2/\omega_1)}{4a} = \Delta S_{\text{isothermal}} \frac{\ln(\omega_2/\omega_1)}{4a} = \frac{\beta^2}{8} (\omega_2^2 - \omega_1^2) \frac{\log(\omega_2/\omega_1)}{4a}. \quad (\text{D7})$$